ELSEVIER

Biochimica et Biophysica Acta 1325 (1997) 41–62

BIOCHIMICA ET BIOPHYSICA ACTA
BBA

Biophysical characterization of cationic lipid:DNA complexes

S.J. Eastman *, C. Siegel, J. Tousignant, A.E. Smith, S.H. Cheng, R.K. Scheule

Genzyme Corporation, One Mountain Road, Framingham, MA 01701-9322, USA

Received 14 August 1996; revised 19 November 1996; accepted 19 November 1996

Abstract

To better understand the structures formed by the interaction of cationic lipids with DNA, we undertook a systematic analysis to determine the biophysical characteristics of cationic lipid:DNA complexes. Four model cationic lipids with different net cationic charge were found to interact in similar ways with DNA when that interaction was compared in terms of the apparent molar charge ratio of lipid to DNA. When DNA was present in charge excess over the cationic lipid, the complex carried a net negative charge as determined by zeta potential measurements. Under these conditions, some DNA was accessible to ethidium bromide, and free DNA was observed in agarose gels and in dextran density gradients. Between a lipid:DNA charge ratio of 1.25 and 1.5:1, all the DNA became complexed to cationic lipid, as evidenced by its inaccessibility to EtBr and its complete association with lipid upon agarose gel electrophoresis and density gradient separations. These complexes carried a net positive charge. The transition between negatively and positively charged complexes a occurred over a very small range of lipid to DNA ratios. Employing a fluorescent lipid probe, the addition of DNA was shown to induce lipid mixing between cationic lipid-containing vesicles. The extent of DNA-induced lipid mixing reached a maximum at a charge ratio of about 1.5:1, the point at which all the DNA was involved in a complex and the complex became positively charged. Together with freeze-fracture electron micrographs of the complexes, these biophysical data have been interpreted in light of the existing models of cationic lipid:DNA complexes.

Keywords: Cationic lipid; Biophysical characterization; Zeta potential; Lipid mixing; Ethidium bromide exclusion; Gradients; Lipid:DNA complex

1. Introduction

The finding that DNA complexed to cationic liposomes can transfect cells efficiently in vitro [1] and in vivo [2–7] has resulted in the evaluation of these lipids for gene therapy applications. Cationic liposome-mediated transfection of many cell types has been demonstrated [8–12] employing a multitude of different cationic lipids [1,8,9,13–16].

Despite the intense interest in these systems, the biophysical characteristics of cationic lipid:DNA complexes have only just begun to be evaluated. Recent studies by Gershon et al. [17] and Jääskeläinen et al. [18] have described some of the characteristics of these complexes, including the ability of DNA and oligonucleotides to induce lipid mixing between cationic lipid vesicles. Several recent reports have

Abbreviations: EtBr, ethidium bromide; DOPE, dioleoylphosphatidylethanolamine; pyrene-PE, 1-hexadecanoyl-2-(1-pyrenedecanoyl)-*sn*-glycero-3-phosphoethanolamine; TOTO-1, benzothiazolium-4-quinolinium dimer; DOSPA 2′-(1″,2″-dioleoyloxypropyldimethyl-ammonium bromide)-*N*-ethyl-6-amidospermine tetra trifluoroacetic acid salt; DMRIE, 1,2-dimyristyloxypropyl-3-dimethyl-hydroxyethyl ammonium bromide; FFEM, freeze-fracture electron micrographs/microscopy

* Corresponding author. Fax: +1 (508) 872 9080.

PII S0005-2736(96)00242-8

described electron micrographs of metal shadowed [17], negatively stained [19,20], and freeze-fractured [21] cationic lipid:DNA complexes, all of which indicate that cationic lipids serve to condense DNA. The ionic interactions between DNA and polycations have been studied by various groups [22–24]. These studies indicate a tight binding of DNA to the polycations employed (including cationic lipids) as observed by various techniques including agarose gel electrophoresis [22,23], DNAse protection [23] and centrifugation [1,24].

Several models of the structure of cationic/lipid DNA complexes have been proposed (for examples see Refs. [13–15,21,22,24–27]). In general, these models fall into two categories based on the relative orientations of the cationic lipid and DNA. In one model, as exemplified by Felgner et al. [28], the DNA binds electrostatically to the outside of the cationic lipid vesicles, i.e., it is adsorbed to the vesicle. In a second model, the cationic lipid 'coats' the DNA in a lipid shell [15,17,21,29]. Mixtures of these two basic models are certainly possible, however, we will restrict our interpretation of the data to these two models, termed *external* or *internal*, as they refer to the position of the DNA relative to the cationic lipid.

We have examined the biophysical characteristics of cationic lipids containing different numbers of positive charges mixed with plasmid DNA as a function of the apparent molar charge ratio. In addition to lipid mixing and ethidium bromide accessibility, we have obtained complementary zeta potential measurements to elucidate the nature of the complexes. These new biophysical data are evaluated critically in terms of the internal and external models of cationic lipid:pDNA complexes and the literature data supporting them.

2. Materials and methods

The neutral lipid dioleoylphosphatidylethanolamine (DOPE) was purchased from Avanti Polar Lipids (Alabaster, AL) and was determined to be $>99\%$ pure by HPLC. The fluorescent lipid 1-hexadecanoyl-2-(1-pyrenedecanoyl)-*sn*-glycero-3-phosphoethanolamine (pyrene-PE) and the fluorescent DNA probe benzothiazolium-4-quinolinium dimer (TOTO-1) were purchased from Molecular Probes (Eugene, OR). Dextran T-500 (ave. M_r 500 000) was purchased from Pharmacia (Uppsala, Sweden). Opti-MEM was from Life Technologies (Grand Island, NY). All other chemicals were purchased from Sigma Chemical Co. (St. Louis, MO).

Four cationic lipids with net positive charges of $+1$, $+2$, $+3$, and $+5$ were chosen to examine the dependence of lipid:DNA complex characteristics on this variable. Cationic lipids *N,N*-dioctadecyllysineamide (lipid 43) and N^1,N^1-dioctadecyl-1,2,6-triaminohexane (lipid 47) were synthesized by Genzyme (Cambridge, MA). 1,2-Dimyristyloxypropyl-3-dimethyl-hydroxyethyl ammonium bromide (DMRIE) and 2′-(1″,2″-dioleoyloxypropyldimethylammonium bromide)-*N*-ethyl-6-amido-spermine tetra trifluoroacetic acid salt (DOSPA) were made by Vical (San Diego, CA). Fig. 1 depicts the structures of the cationic lipids used in this study. All experiments were performed employing the cationic lipids formu-

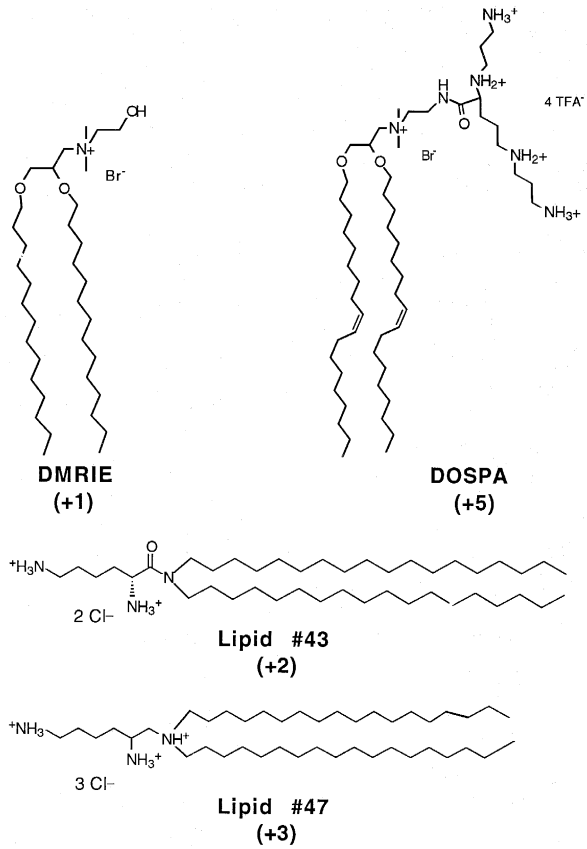

Fig. 1. Structures of cationic lipids used in this study.

lated with the neutral co-lipid DOPE at a 1:1 molar ratio. The lipids were dissolved in $CHCl_3$, mixed with an equimolar amount of DOPE (in $CHCl_3$) and dried down to a thin film under a stream of nitrogen. Residual $CHCl_3$ was removed under high vacuum for 1 h. The lipid films were stored frozen at −20°C.

2.1. Synthesis of N,N-dioctadecyllysineamide (lipid 43)

N,N-Dioctadecylamine (1.35 g, 2.58 mmol, Fluka) and L-*Nα,Nε*-diBOClysine *N*-hydroxysuccinimide ester (1.0 g, 2.58 mmol, Sigma) were combined in 15 ml of methylene chloride and 2 ml triethylamine was added. The reaction mixture was heated briefly to effect complete dissolution and then stirred at ambient temperature overnight. Water (20 ml) and methylene chloride (50 ml) were added to the reaction mixture and the layers were separated. The aqueous fraction was extracted a second time with 50 ml methylene chloride. The combined organic fractions were dried over $MgSO_4$, filtered and concentrated in vacuo. The residue was purified by column chromatography (150 g silica gel; eluant-hexane:ethyl acetate 8:2). The purified material, *N,N*-dioctadecyl-*Nα,Nε*-diBOClysineamide (1.59 g), was dissolved in 25 ml of chloroform and stirred for 2 h while HCl gas was bubbled through the solution. This solution was purged with N_2 gas and concentrated in vacuo. Compound 43 (1.34 g) was obtained in 68% yield. The structure of the lipid was confirmed by ^{1}H-NMR.

2.2. Synthesis of N^1,N^1-dioctadecyl-1,2,6-triaminohexane (lipid 47)

To *N,N*-dioctadecyl-*Nα,Nε*-diBOClysineamide (760 mg, 0.823 mmol) in 30 ml anhydrous tetrahydrofuran stirred at ambient temperature was added $LiAlH_4$ (185 mg, 4.87 mmol) in portions. The reaction mixture was stirred at ambient temperature overnight under a nitrogen atmosphere. The reaction was quenched by the dropwise addition of 2 ml water and the resulting solution was concentrated in vacuo. To this residue was added in order 10 ml of 1 M HCl, 50 ml of methylene chloride, and 10 ml of 1 M NaOH (final pH = 10). The layers were separated and the aqueous fraction was extracted a second time with 50 ml of methylene chloride. The combined organic layers were dried over $MgSO_4$ and filtered. The filter cake was washed with 50 ml of methylene chloride. The combined filtrates were concentrated in vacuo to give 700 mg of crude product. The crude product was purified by column chromatography (80 g silica gel; eluant-hexane:ethyl acetate 7:3). Fractions containing the purified product were combined and concentrated in vacuo to obtain 490 mg of the product protected as the diBOC derivative. To 200 mg of this diBOC derivative were added 4 ml of chloroform and 1 ml of trifluoroacetic acid. The resulting reaction mixture was stirred at ambient temperature for 2h and concentrated in vacuo . The residue was dissolved in 25 ml of water and 25 ml of methylene chloride and adjusted to pH 10 with approximately 2 ml of concentrated ammonium hydroxide. The layers were separated and the aqueous layer extracted a second time with 25 ml of methylene chloride. The organic fractions were combined, dried over Na_2SO_4 and concentrated in vacuo. The resulting residue was dissolved in 10 ml of diethyl ether, HCl gas was bubbled through the solution for 2 min and the solution was cooled at 4°C overnight. The precipitated product was collected by filtration, washed with cold (4°C) diethyl ether, and dried under vacuum to obtain 160 mg of compound 47 in 67% yield. The structure of the lipid was confirmed by ^{1}H-NMR.

2.3. Preparation and characterization of cationic liposomes

Cationic lipid:DOPE (1:1) vesicles were prepared at concentrations between 1 and 5 mM cationic lipid by adding distilled water (dH_2O) to the lipid films and vortexing for 2 min. Typically, vesicle sizes were determined within 1 h of their preparation. DMRIE vesicles produced in this manner had a mean diameter of approximately 450 nm, (range 200–600 nm) as determined by photon correlation spectroscopy (PCS) and freeze-fracture electron microscopy. Lipid 43 and lipid 47 lipid produced similarly-sized vesicles; mean vesicle diameters were 450 and 500 nm, respectively. DOSPA produced vesicles that were significantly smaller than observed for the other cationic lipids; the majority ($\approx$ 85%) had a mean diameter of 120 nm with a smaller population ($\approx$ 15%) of larger vesicles (mean diameter 412 nm).

The sizes of cationic lipid:pDNA complexes were also determined; sizes were determined within 30 min. of preparation. In general, lipid:pDNA complexes prepared at low lipid:pDNA charge ratios ($<1:1$) had mean diameters that were approximately the same or smaller than the corresponding vesicles alone. For example, at a charge ratio of 0.50:1, two populations of DMRIE complexes with mean diameters of 213 ($\approx 37\%$) and 424 nm (63%) respectively, were observed by PCS. Similar-sized complexes were observed for lipid 43 vesicles, except that the proportion of complexes in each size group was reversed (i.e., 67% at 266 nm and 37% at 750 nm). Complexes produced from lipid 47 at this charge ratio had a mean diameter of 324 nm (83%) with a small population of large complexes of approximately 1 μm in size. DOSPA vesicles produced small complexes at this charge ratio, with about 91% of the complexes having a mean diameter of 126 nm. For all the lipids employed, the maximum complex sizes (typically around 1 μm with particles ranging from 500 nm to several μm; DOPSA:DOPE/DNA complexes were smaller with maximal mean sizes of approximately 300 nm) occurred at a charge ratio between 1.0 and 1.5:1, where the complexes were net neutral. Smaller complexes were again observed at charge ratios where the complexes became positively charged.

2.4. Plasmid DNA

pCMV-βGal (Clontech, Palo Alto, CA) was grown in *Escherichia coli* and purified employing 'Megaprep' columns (Qiagen) according to the manufacturer's instructions. The plasmid concentration was determined by A_{260} measurements. Plasmid purity was assessed using agarose gel electrophoresis and A_{260}/A_{280} ratios. All plasmid preparations showed a major band of closed circular DNA of the expected size and a minor amount ($<25\%$) of nicked plasmid on gels. Only plasmid preparations with A_{260}/A_{280} ratios ≥ 1.8 were utilized. Endotoxin was measured employing a Limulus Amebocyte Lysate test (Bio-Whittaker, Walkersville. MD). DNA preparations containing endotoxins at levels >5 E.U./mg of plasmid DNA were extracted with Triton X-114 [30] to reduce the endotoxin load below this level. DNA concentrations given are based on an average nucleotide molecular mass of 330.

2.5. Freeze-fracture electron microscopy

Freeze fracture electron microscopy of lipid:DNA complexes was performed by Northern Lipids (Vancouver, B.C., Canada). DMRIE:DOPE:DNA complexes were prepared at lipid:DNA charge ratios of 0.25, 0.50, 0.75, 1.5, and 2.5:1 by adding an equal volume (125 μl) of DNA at the appropriate concentration to tubes containing 1 mM cationic lipid. Addition of the DNA was performed by pipetting the DNA rapidly into the lipid sample (<5 s), while drawing the pipet tip up through the lipid suspension. After addition of the DNA, the complex was allowed to incubate at room temperature for 10 min. before glycerol was added to a final concentration of 33% v/v and allowed to equilibrate. Samples were frozen in Freon 22 cooled by liquid nitrogen and fractured (Balzers apparatus). Platinum/carbon replicas of the samples were prepared as previously described [31]. Electron microscopy was performed on a Phillips electron microscope operating at 80 kV.

2.6. Zeta potentials

Zeta potentials were measured (5 measurements per sample) with a Malvern Zetasizer 4 (Malvern Instruments, Southborough, MA) in a zeta cell (AZ-104 cell, Malvern Instruments). Dried lipid films containing the cationic lipid and DOPE were hydrated in dH_2O. DNA typically was diluted to a concentration of 300 μM in dH_2O. The DNA solution (1.5 ml) was added to an equal volume of cationic lipid vesicles and incubated at room temperature for 10 min. Enough NaCl (4 mM) was added to result in a final concentration of 1 mM NaCl. If necessary, the sample was diluted further with 1 mM NaCl to maintain a photomultiplier signal below 4000 counts per second. For samples analyzed in Opti-MEM, $10\times$ Opti-MEM was added to the sample after the initial 10-min incubation period. Any further dilution was done with $1\times$ Opti-MEM.

2.7. Agarose gel electrophoresis

Cationic lipid:DNA complexes (2 μg DNA/sample) were prepared at the desired lipid:DNA ratios in 20 μl. After a 10-min incubation at room temperature, 5 μl of $5\times$ Orange G running buffer (25%

sucrose in dH_2O, Orange G (Sigma) to color) was added to each sample, followed by a brief vortexing. Samples were electrophoresed on 0.75% agarose (SeaKem ME, FMC BioProducts, Rockland, ME) gels containing 1 μg/ml ethidium bromide (EtBr) in Tris-borate EDTA buffer (TBE), pH 8.0 containing 0.5 μg/ml EtBr at 100 V for 1 h. The EtBr-stained DNA bands were visualized and photographed on an ultraviolet transilluminator (Fotodyne, New Berlin, WI).

2.8. Ethidium bromide exclusion

To determine the effect of the EtBr:nucleotide ratio on the profile of EtBr fluorescence obtained in the presence of cationic lipids, standard curves were generated at EtBr:nucleotide ratios of 1:6 and 1:50 (mol:mol). DNA was added to test tubes in triplicate in 1.5 nmol (by nucleotide) increments and brought up to a final volume of 500 μl with dH_2O (a range of 0–30 μM). Five hundred μl of a 5 or 0.6 μm EtBr stock solution was then added to each tube at EtBr:nucleotide ratios of 1:6 or 1:50 respectively. The resulting fluorescence was measured in a spectrofluorometer (Spex Fluoromax), using an excitation wavelength of 260 nm, an emission wavelength of 591 nm, and a 500 nm emission cutoff filter.

The ability of the cationic lipid DMRIE to prevent EtBr intercalation into DNA was assessed at 2.5 μM and 0.3 μM EtBr. DMRIE:DOPE vesicles were diluted to a concentration of 100 μM DMRIE in dH_2O. Fifty μl of 300 μM DNA was added to 450 μl of dH_2O containing 0 to 60 μM cationic lipid (final concentration). Blanks containing no lipid or no DNA were also prepared. The mixtures were incubated for 10 min at room temperature and then 0.5 ml of the appropriate EtBr solution containing either 5.0 μM EtBr (1 EtBr/6 nucleotides) or 0.6 μM EtBr (1 EtBr/50 nucleotides) was added to each tube, briefly vortexed, and incubated at room temperature for another 10 min. The fluorescence of each sample was corrected for the background fluorescence of EtBr in the absence of DNA and then normalized to the EtBr fluorescence of 15 μM DNA in the absence of lipid. The ability of other model cationic lipids to prevent EtBr intercalation was assessed at an EtBr:nucleotide ratio of 1:6 as described above for DMRIE.

The effect of ionic strength on the ability of cationic lipid vesicles to prevent EtBr intercalation was assessed at a 1:6 EtBr:nucleotide molar ratio as described above, except that the complexes were prepared in solutions of varying ionic strength. Briefly, stock dispersions of cationic lipid vesicles in dH_2O were diluted in saline of variable ionic strengths (dH_2O, 20 mM NaCl, 150 mM NaCl, or 1.5 M NaCl) and then diluted further in these buffers to the desired concentration. After adding DNA, the mixtures were incubated for 10 min at room temperature and then the appropriate salt solution containing EtBr was added to each tube, briefly vortexed, and incubated at room temperature for another 10 min. before measuring the fluorescence. The fluorescence of each sample was corrected for the background fluorescence and normalized as described above.

2.9. Lipid mixing

DNA-induced mixing of lipids between vesicles was monitored using pyrene-PE [32,33]. Excitation of pyrene excimers at 340 nm leads to emission at 482 nm, 100 nm higher than the emission wavelength of the excited monomer (383 nm). Excimer formation in the lipid vesicles is proportional to the density of pyrene-PE. Therefore any lipid mixing between labeled vesicles and unlabeled vesicles (present in a 10-fold excess) results in dilution of the pyrene-PE, a decrease in the excimer fluorescence and a corresponding increase in monomer fluorescence.

A standard curve of the excimer/monomer fluorescence ratio as a function of the percentage of pyrene-PE was generated. Cationic vesicles containing between 2 and 10 mol% pyrene-PE were hydrated in dH_2O and then diluted with dH_2O to give the same total amount of pyrene-PE in each sample. Emission spectra of the pyrene fluorescence (Ex 340 nm, Em 360–550 nm, 1.5 nm bandpass) were obtained and a standard curve prepared from the relative excimer and monomer fluorescence intensities at 482 and 383 nm, respectively. The ratio of excimer/monomer fluorescence was linear over the concentration range of pyrene-PE employed (2 to 10 mol%) for each of the cationic lipids studied. At 10 mol% pyrene-PE, the excimer:monomer ratio was ≈ 0.4 for the cationic lipids DMRIE, 43 and 47, and ≈ 0.2 for DOSPA:DOPE vesicles. A linear decrease

in the ratio was observed with decreasing percentages of pyrene-PE in each of the model cationic vesicles.

Final equilibrium values of lipid mixing were obtained in triplicate by adding 100 μl of lipid vesicles (10% of the vesicles were labeled with 10 mol% pyrene-PE) to 1.35 ml of dH_2O to result in a final concentration of 10 μM cationic lipid. Fifty microliters of DNA at the appropriate concentration to obtain the desired lipid:DNA charge ratio was then added to each tube and the samples incubated for 10 min at room temperature. In addition, one set of samples was incubated with 50 μl of dH_2O (maximal excimer:monomer ratio) and one set with 50 μl of 1 M octylglucoside (100% lipid mixing). The excimer:monomer fluorescence ratios for each sample were then measured employing a constant wavelength analysis program on the spectrofluorometer.

Control experiments were performed to determine the effects of changes in the lipid phase (e.g., production of the hexagonal H_{II} phase) or other environmental factors on the excimer:monomer ratio. For each of the four cationic lipids, labeled vesicles in the absence of unlabeled acceptor vesicles (1 μM cationic lipid) were incubated at the same lipid:DNA ratios used in the mixing experiments. After a 10-min incubation at room temperature, the excimer:monomer ratio was determined. Changes in the ratio were observed, typically corresponding to a calculated maximal extent of lipid mixing of $< 10\%$, compared to $\approx 85\%$ for the case where acceptor vesicles were present. For DOSPA:DOPE, the calculated maximal extent of lipid mixing under these conditions was $\approx 7\%$ compared to $\approx 55\%$ in the presence of acceptor vesicles. The resonance energy transfer probes rhodamine-PE and NBD-PE were not employed, because it was shown in preliminary experiments that cationic lipids significantly quenched the fluorescence of both lipids (data not shown).

2.10. Kinetics of lipid mixing

The kinetics of lipid mixing induced by DNA were examined for each of the cationic lipids as a function of the cationic lipid:DNA ratio. Cationic vesicles labeled with 10 mol% pyrene-PE were diluted to 30 μM cationic lipid in dH_2O. Unlabeled vesicles were diluted to 270 μM cationic lipid in dH_2O. Fifty μl of the labeled and unlabeled vesicles were then added to a stirred cuvette containing 1.35 ml of dH_2O to give final lipid concentrations of 1 μM labeled and 9 μM unlabeled vesicles. After monitoring the excimer/monomer ratio for 50 s, 50 μl of a DNA solution of the appropriate concentration to yield the desired lipid:DNA ratio was added to the cuvette through an injection port and the excimer/monomer ratio of the fluorescence was monitored for approximately 3 min. Fifty μl of 1 M octylglucoside (final concentration = 32.3 mM) was then injected to disrupt the complex and provide a fluorescence ratio characteristic of totally mixed lipid.

2.11. Dextran step gradient separations

A stock solution of 30% (w/v) Dextran T-500 was prepared in dH_2O. This stock solution was used to prepare concentrations of Dextran ranging from 5% to 20% w/v containing 5 μg/ml EtBr. Two ml aliquots of these Dextran solutions were layered in centrifuge tubes (Beckman Ultraclear; 14×89 mm) in the following order: 30%, 20%, 15%, 10% and 5% Dextran. Because the amount of cationic lipid required to prepare a complex of a given charge ratio is inversely related to the net charge of the lipid, cationic lipid:DNA complexes were labeled with 5 (DMRIE), 10 (lipid 43) 15 (lipid 47) or 20 (DOSPA) mol% pyrene-PE to total lipid to maintain the same total amount of label between cationic lipid samples for visualization purposes. Complexes were prepared at the desired lipid:DNA ratios and at a final DNA concentration of 150 μM. Five-hundred-μl aliquots were layered on top of the 5% Dextran layer. Gradients were centrifuged at 40 000 rpm for 1 h (4°C) in a Beckman SW41 rotor. The bands were observed with a long-wavelength UV light (366 nm) positioned slightly above and in front of the tubes at an angle of about 45 degrees. The sample tubes were photographed against a black backdrop using Kodak Ektachrome 100 film.

3. Results

3.1. Freeze-fracture electron microscopy

Freeze-fracture electron micrographs (FFEM) of DMRIE:DOPE complexed with DNA were prepared

using samples formed as a function of the molar ratio of cationic lipid to DNA. Fig. 2 shows that at low lipid:DNA ratios, the complexes were relatively small and homogeneous in size (200–500 nm on average); complexes formed at a charge ratio of 0.75:1 were the smallest and most homogeneous in nature. At charge ratios of 1.5:1 and above, the complexes were much larger (200 nm to > 2 μm) and significantly more heterogeneous. At all charge ratios, the liposomes in complexes appeared fundamentally different from free liposomes, namely, the liposomes in complexes appeared to be compressed or compacted as if the aqueous contents had been lost. Although the pDNA was not visible by this technique, these results suggest that the DNA may affect the packing and perhaps even the phase of the lipid in the complex.

3.2. Zeta potentials

Zeta potentials of lipid:DNA complexes were measured in 1 mM NaCl as a function of the lipid:DNA ratio for the four model cationic lipids. Fig. 3 shows that the zeta potentials of the complexes of the cationic lipids did not all correlate in the same way with the molar ratio of cationic lipid:DNA in the complex (Fig. 3A). However, the zeta potentials of all the cationic lipids were found to have a similar functional dependence when plotted against the apparent charge ratio of cationic lipid to DNA (Fig. 3B). For example, twice as much DMRIE ($+1$ charge/lipid) was required to induce changes in the zeta potential similar to those seen when using lipid #43 ($+2$ charge/lipid).

The zeta potentials of all the complexes were negative until a charge ratio of approximately 1.25:1 was obtained (Fig. 3B). DMRIE, #43 and DOSPA complexes became positively charged at this charge ratio while lipid #47:DNA complexes maintained a negative charge even at a charge ratio of 1.5:1. For all the cationic lipids employed, the transition from negatively to positively charged complexes occurred over a very small increment in the charge ratio of cationic lipid to DNA, i.e., ≈ 0.25. At charge ratios greater than ≈ 1.75:1, all complexes exhibited positive zeta potentials that were essentially those of the cationic liposomes in the absence of DNA. The apparent requirement for a higher charge ratio for lipid 47 (compared to the other lipids) to produce a lipid:DNA complex with a positive zeta potential may reflect an effective charge of somewhat less than 3 positive charges/lipid due to the inability of all the potential cationic charges on lipid 47 to interact with the DNA, perhaps due to a pK_a of the innermost nitrogen below pH 7 (not measured) or because of steric hindrance (see Fig. 1).

For DMRIE and DOSPA, zeta potentials were also determined in Opti-MEM, a physiologic medium in which lipid:DNA complexes often are placed on cells for in vitro transfections. Fig. 4 shows that the zeta potential profiles of the complexes as a function of lipid to DNA charge ratio were significantly different in Opti-MEM and 1 mM NaCl. Zeta potentials of the complexes in Opti-MEM were significantly more negative than those measured in 1 mM NaCl at all ratios of cationic lipid:DNA (Fig. 4). This result was unexpected for ratios < 1, since one might predict that salt would shield the negative charges on the surface of the DNA and result in less negative zeta potentials. Indeed, the zeta potential of an anionic polystyrene bead standard (AZ-55; Malvern Instruments) was found to be significantly less negative in Opti-MEM than in 1 mM NaCl, -39 and -50 mV, respectively. Consistent with the shielding expected in higher salt, the cationic liposomes alone exhibited a smaller positive zeta potential in Opti-MEM compared to 1 mM NaCl (Fig. 4). In 1 mM NaCl, DMRIE and DOSPA complexes exhibited positive zeta potentials above charge ratios of 1.25:1. In Opti-MEM, this crossover point was shifted to higher lipid:DNA ratios. DMRIE complexes attained a positive zeta potential at charge ratios ≥ 2.0:1, while DOSPA complexes remained negatively charged up to a charge ratio of ≥ 2.5:1.

3.3. Agarose gel electrophoresis

Agarose gel electrophoresis of cationic lipid:DNA complexes was used to assess the relative amounts of DNA that were free or incorporated into the complex as a function of the lipid:DNA ratio. DNA in a lipid complex did not migrate out of the well under these conditions. This was most likely the result of size exclusion, rather than charge neutralization, as shown by the inability of cationic liposomes alone (containing a fluorescently-labeled cationic lipid) to migrate into the gel (data not shown). Fig. 5 shows that the

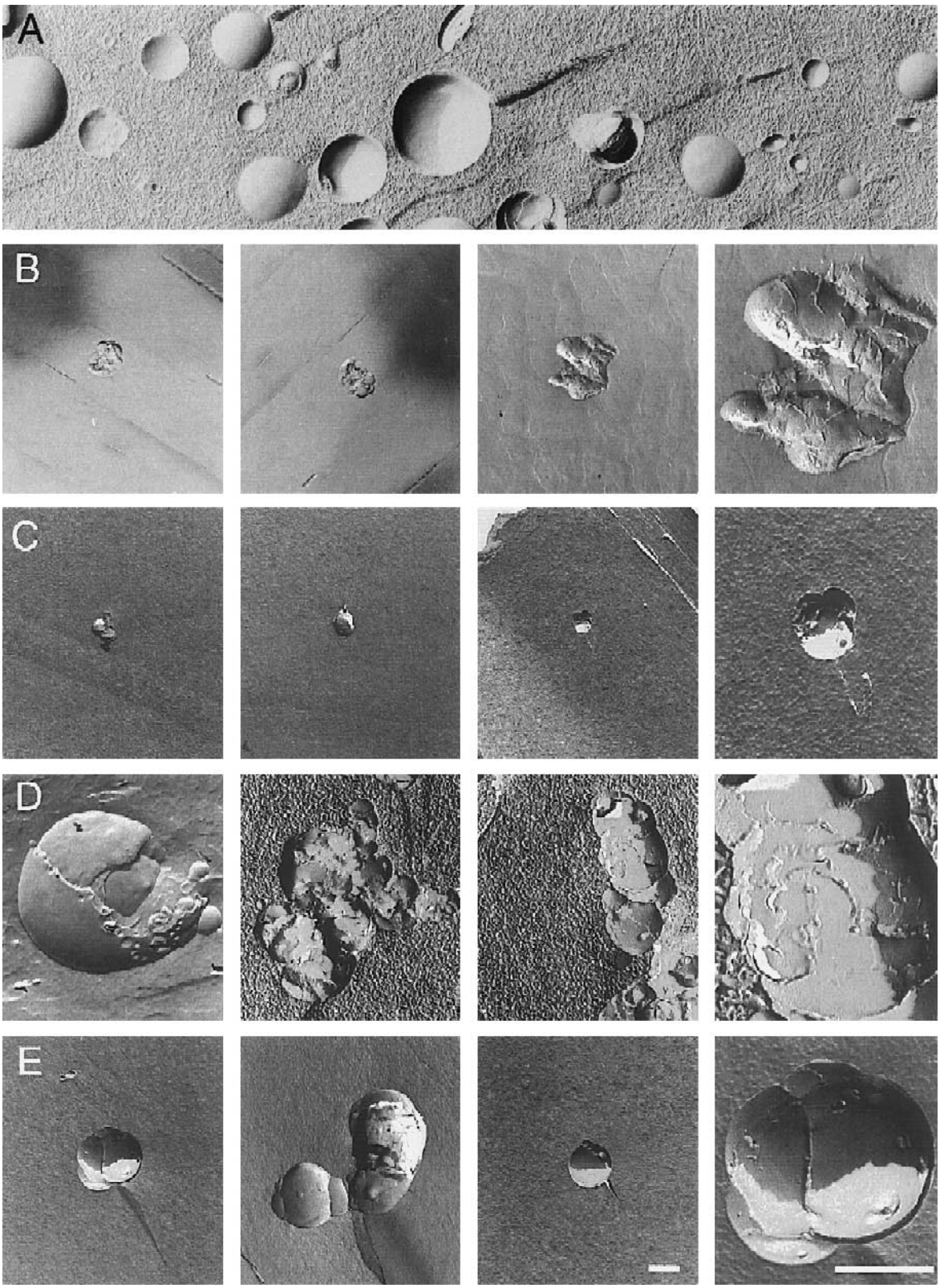
A
B
C
D
E

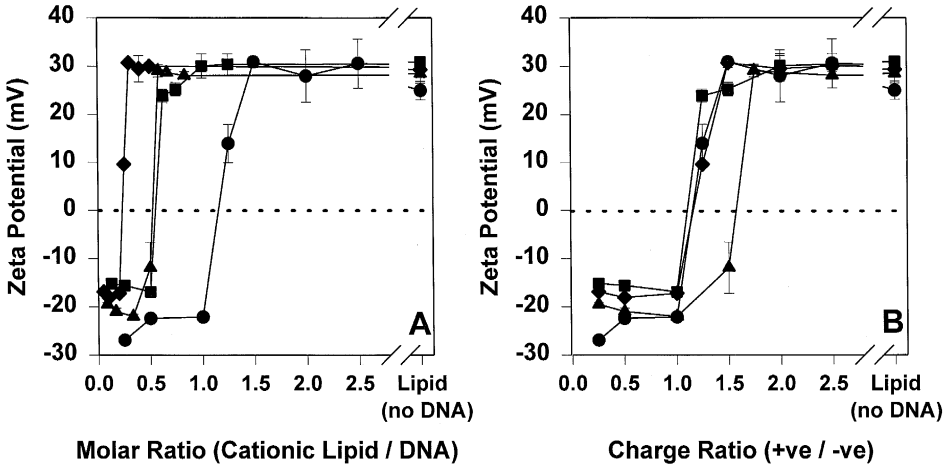

Fig. 3. Zeta potentials of lipid alone (no DNA) and lipid:DNA complexes in 1 mM NaCl. Cationic lipid vesicles were prepared as 1:1 molar ratios of cationic lipid:DOPE and mixed with DNA at various ratios. Cationic lipids and their apparent charges are: DMRIE (●, +1), #43 (■, +2), #47 (▲, +3) and DOSPA (◆, +5). Zeta potentials are plotted as a function of (A) the molar ratio and (B) the apparent charge ratio of the cationic lipid:DNA. Error bars represent standard deviations.

amount of uncomplexed, or free DNA decreased as the ratio of lipid:DNA was increased. A corresponding ratio-dependent increase in the amount of complexed DNA was observed. These results are consistent with previous reports that employed agarose gel electrophoresis to examine cationic lipid [23] and lipopolylysine:DNA complexes [34].

The charge ratio of cationic lipid:DNA required to completely complex the DNA varied between the cationic lipids. For DMRIE and DOSPA, all of the DNA was complexed at charge ratios $\geq 1.25:1$, corresponding to the point at which these complexes attained a positive zeta potential (see Fig. 3). For lipid #43, some free DNA was observed at a charge ratio of 1.25:1. This was somewhat surprising since this lipid had a positive zeta potential at this charge ratio (see Fig. 3). However, since the transition between negatively and positively charged complexes occurs between charge ratios of 1.0 and 1.25:1, a small variation in the addition of either the lipid or DNA could account for the presence of free DNA in this sample. Indeed, subsequent analysis with this lipid showed that all the DNA was bound at charge ratios $\geq 1.25:1$ (not shown). For lipid #47, free DNA was observed in the agarose gel until a charge ratio of 1.50:1 was reached. This result compares favorably to that obtained in the zeta potential experiments which indicated that for lipid #47 a charge ratio of 1.75:1 was required to produce a complex with an overall positive charge (see Fig. 3). Overall, the amount of DNA complexed was found to be dependent on the charge ratio of the cationic lipid:DNA and independent of the identity of the cationic lipid.

3.4. EtBr exclusion

Another approach used to characterize cationic lipid:DNA complexes was to examine the ability of cationic lipids to prevent ethidium bromide intercalation into DNA. EtBr fluorescence is enhanced approximately 40-fold upon intercalation into DNA. In

Fig. 2. Freeze-fracture electron micrographs of DMRIE:DOPE:DNA complexes prepared at various ratios of cationic lipid to DNA. (A) DMRIE:DOPE (1:1) vesicles in the absence of DNA. Complexes prepared at cationic lipid:DNA molar ratios of (B) 0.50:1, (C) 0.75:1, (D) 1.5:1 and (E) 2.5:1. The first three panels from each row show representative complexes from the samples listed above, all at the same magnification. The final panel of each row shows a magnified view of the complexes produced at each lipid:DNA ratio. Scale bars represent 200 nm.

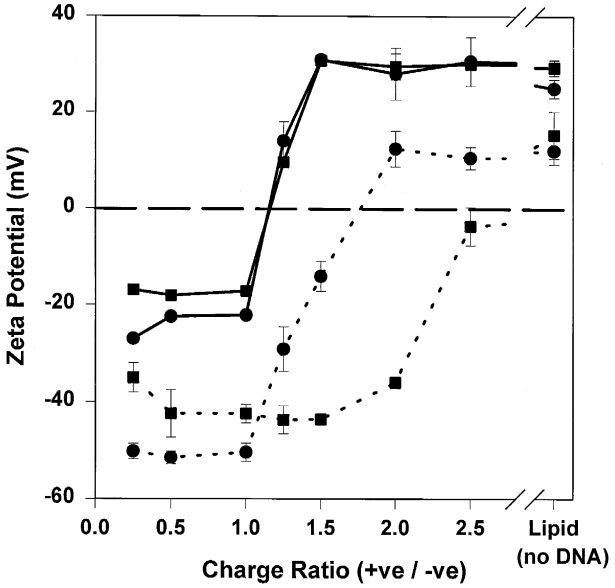

Fig. 4. Zeta potentials of DMRIE:DOPE and DOSPA:DOPE lipid vesicles (no DNA) and lipid:DNA complexes in 1 mM NaCl and Opti-MEM as a function of the charge ratio of the cationic lipid:DNA. DMRIE (●) and DOSPA (■) in 1 mM NaCl (solid lines) and Opti-MEM (dashed lines). Error bars represent standard deviations.

general, as the ratio of cationic lipid to DNA was increased, the EtBr fluorescence decreased, indicating that less DNA was accessible to EtBr. However, these decreases in fluorescence intensity with increasing lipid:DNA ratio were found to be markedly dependent on the concentration of EtBr relative to DNA. At 2.5 μM EtBr, Fig. 6A shows that decreases in EtBr fluorescence were directly proportional to the amount of cationic lipid added to a constant amount of DNA (15 μM), while at 0.3 μM EtBr, the decrease in fluorescence with cationic lipid:DNA charge ratio had a sigmoidal profile.

The origins of these differences were investigated by titrating a constant concentration of EtBr (2.5 μM or 0.3 μM) with increasing concentrations of free (uncomplexed) DNA. Fig. 6B shows that at 2.5 μM EtBr, increases in fluorescence were linear up to 15 μM DNA. However, Fig. 6C shows that at 0.3 μM EtBr, the EtBr fluorescence reached a maximal value at ≈ 4 μM DNA and then decreased to a relatively constant plateau value at higher DNA concentrations. Thus, because of the equilibria involved, the fluorescence of EtBr intercalated into DNA was linear only if the ratio of EtBr to nucleotides was greater than some minimum value, in this study, 1 EtBr per 6 nucleotides. As the DNA concentration was increased at lower concentrations of EtBr (Fig. 6C), all of the available free EtBr became intercalated and a maximum in the fluorescence was reached.

These results with free DNA were reproduced with the complex. Fig. 6A shows that at 0.3 μM EtBr and 15 μM DNA, where *all* of the EtBr is intercalated according to Fig. 6C, increasing the concentration of cationic lipid (decreasing the concentration of free pDNA) resulted in little change in fluorescence until it decreased precipitously at ≈ 13 μM cationic lipid. This point presumably corresponds to a free DNA concentration of ≈ 3 μM according to Fig. 6C. Titration of DNA with cationic lipid in the presence of excess EtBr (≥ 1 EtBr/6 nucleotides) leads to a *linear* decrease in fluorescence, indicating a gradual reduction in the concentration of free DNA. Titration of DNA with cationic lipid using a limiting EtBr concentration (≤ 1 EtBr/50 nucleotides) leads to a sigmoidal profile (Fig. 6A; as seen by Gershon et al. [17]) that can lead to erroneous interpretations.

In agreement with the zeta potential and agarose gel results, the EtBr exclusion results indicated that the degree of inhibition of EtBr intercalation did not correlate with the molar ratio of cationic lipid:DNA, but rather correlated with the charge ratio of lipid to DNA. For example, Fig. 7A shows that it takes approximately one-fifth the amount of DOSPA ($+5$) as it does DMRIE ($+1$), i.e., 5 μM versus 25 μM respectively, to totally exclude EtBr. Fig. 7B shows that these two lipids are equally effective at excluding EtBr when compared on a charge ratio basis. Slightly more lipid #47 was required to exclude all the EtBr, in agreement with the results of the previous experiments. For all the lipids, a slight apparent excess of positive charge was found to be required to completely inhibit EtBr intercalation.

The effect of ionic strength on the ability of a cationic lipid (DMRIE) to prevent EtBr intercalation into DNA was also examined. Fig. 8 shows that the fraction of the DNA that remained accessible to EtBr increased with increases in the ionic strength. In water, titration with cationic lipid resulted in almost 100% of the DNA becoming inaccessible to EtBr at charge ratios > 1.5, as reflected by the decaying fluorescence signal. In 20 or in 150 mM NaCl, Fig. 8

shows that ≈24% or ≈55%, respectively, of the DNA remained accessible to EtBr at high charge ratios. Identical curves were obtained when the complex was formed in 150 mM NaCl or when it was formed in water and the salt concentration adjusted to 150 mM prior to adding EtBr (data not shown). Complexes prepared in Opti-MEM produced profiles identical to those seen employing 150 mM NaCl, indicating that the observed effect was due mainly to the ionic strength of the suspension, and not to factors such as pH (data not shown). Finally, in 1.5 M NaCl, the DNA was totally accessible to EtBr at all cationic lipid:DNA charge ratios.

3.5. DNA-induced lipid mixing

To determine if DNA could cause mixing of phospholipids between cationic vesicles, a fluorescent lipid was used to probe lipid mixing as a function of the cationic lipid:DNA charge ratio. In a bilayer, pyrene-PE exists in a concentration-dependent excimer–monomer equilibrium [33]. Dilution of pyrene-PE results in a decrease in excimer fluorescence that can be used to monitor lipid mixing. Pyrene-PE was incorporated into donor vesicles at 10 mol% of total lipid and the vesicles were mixed with a ten-fold excess of unlabeled vesicles. Fig. 9A shows that as measured by the pyrene-PE excimer:monomer ratio, the addition of DNA caused substantial lipid mixing between donor and acceptor vesicles, consistent with previously published results [18]. The majority of lipid mixing occurred in the first 30 s after DNA addition. The rate of lipid mixing was very similar for all lipids and charge ratios employed (data not shown); only the final extent of mixing varied significantly.

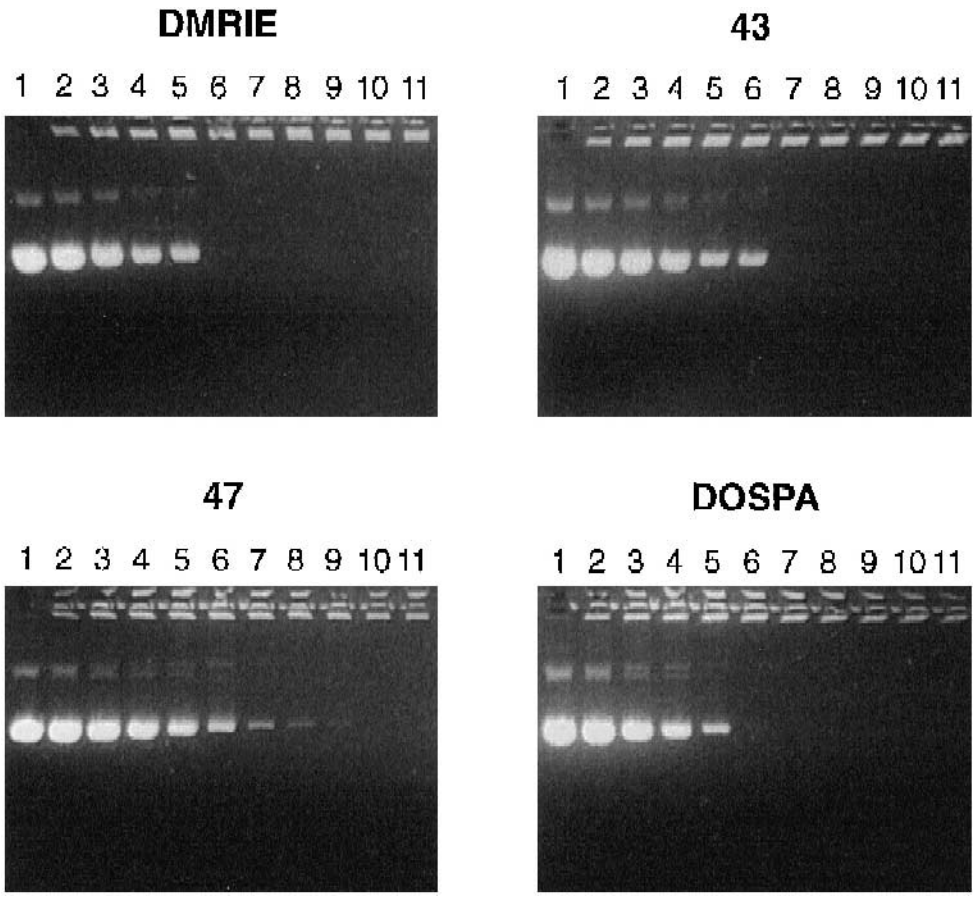

Fig. 5. Agarose gel electrophoresis of cationic lipid:DNA complexes formed at equivalent charge ratios. See Methods for additional details. The wells contain lipid and DNA at the following charge ratios (left to right): 0, 0.25, 0.50, 0.75, 1.00, 1.25, 1.50, 1.75, 2.00, 2.25 and 2.50.

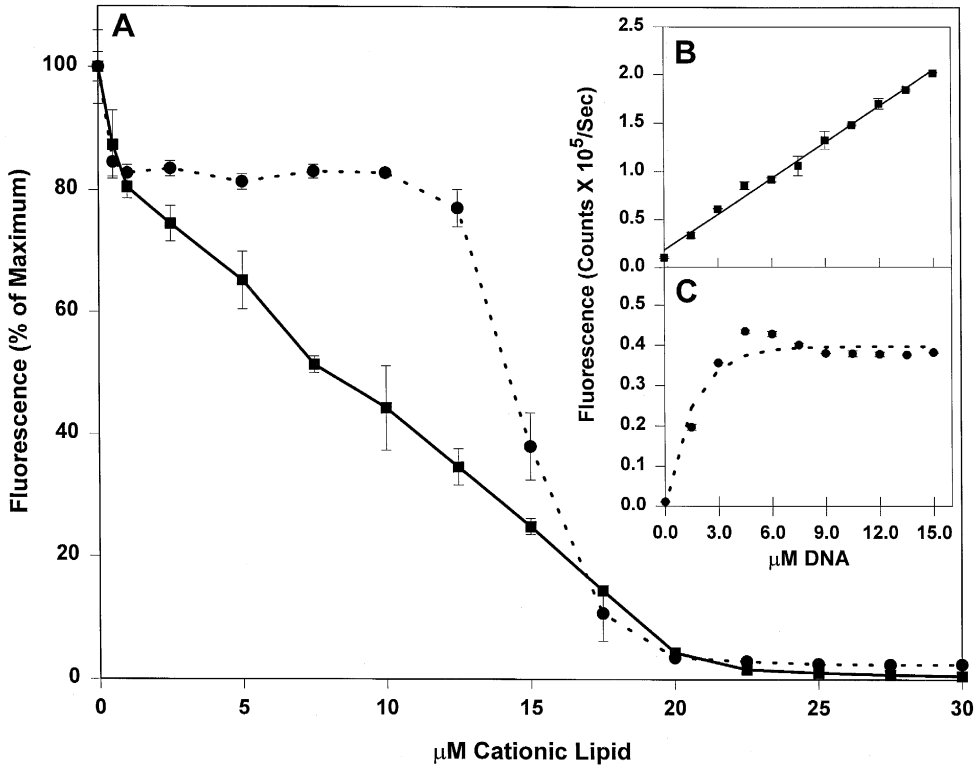

Fig. 6. Effect of the EtBr:DNA ratio on EtBr fluorescence in the presence of cationic lipid. (A) EtBr fluorescence in the presence of 15 μM DNA as a function of the amount of cationic lipid present (0–30 μM DMRIE) and employing either 0.3 μM EtBr (●) or 2.5 μM EtBr (■). Standard curves of EtBr fluorescence versus [DNA] employing (B) 2.5 μM EtBr, and (C) 0.3 μM EtBr. Error bars represent standard deviations.

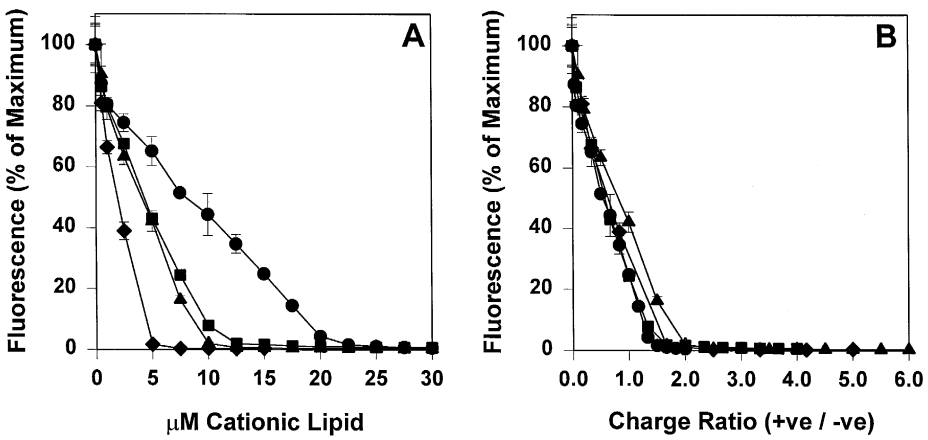

Fig. 7. Effect of cationic lipids on EtBr fluorescence in the presence of 15 μM DNA in dH_2O. (●) DMRIE, (■) #43, (▲) #47, (♦) DOSPA. The fluorescence of 2.5 μM EtBr as a function of (A) the molar ratio and (B) the charge ratio of cationic lipid:DNA. Error bars represent standard deviations.

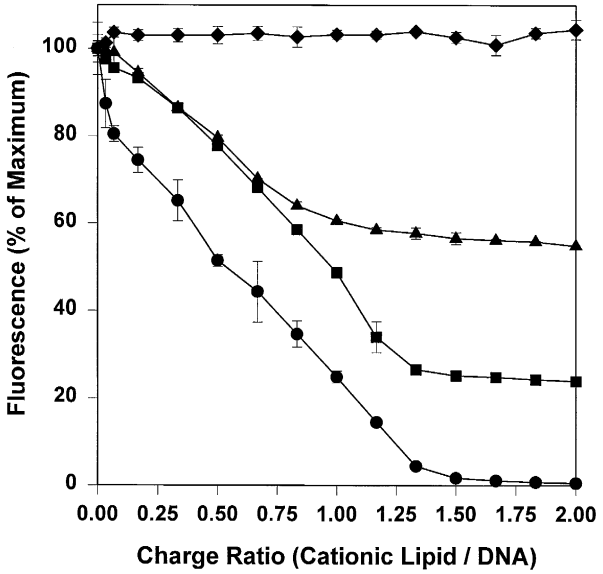

Fig. 8. Effect of ionic strength on EtBr fluorescence in the presence of 15 μM DNA and various amounts of DMRIE:DOPE vesicles. (●) dH_2O, (■) 20 mM NaCl, (▲) 150 mM NaCl, (♦) 1.5 M NaCl. Error bars represent standard deviations.

Fig. 9B and C show that the extent of DNA-induced lipid mixing did not correlate with the molar ratios of the components but rather correlated with the apparent charge ratio of cationic lipid to DNA. DMRIE, #43 and #47 exhibited similar final extents of lipid mixing ($\approx$ 85%). DOSPA vesicles underwent less extensive lipid mixing ($\approx$ 55%) compared to the other cationic lipid vesicles. For lipid vesicles containing DMRIE, #43, and DOSPA, maximal lipid mixing occurred when the charge ratio approached 1.5:1. For cationic lipid #47, maximal lipid mixing occurred at a slightly higher charge ratio of lipid to DNA ($\approx$ 1.75:1). These results are in agreement with the gel electrophoresis, EtBr exclusion and dextran gradient results which indicate that lipid 47 is slightly less efficient than the other cationic lipids at complexing DNA and that the effective charge on lipid #47 may be slightly less than its theoretical charge of $+3$/lipid.

3.6. Dextran density gradients

Lipid:DNA complexes were characterized by separating them from free lipid and DNA on Dextran T-500 sedimentation velocity step gradients. Lipid was labeled with pyrene-PE (blue fluorescence) and DNA with EtBr (red fluorescence). Free DNA and lipid banded on top of the 5% Dextran layer (not shown). Fig. 10 shows that the addition of DMRIE vesicles to DNA resulted in the formation of complexes that banded on top of the 15% and 20%

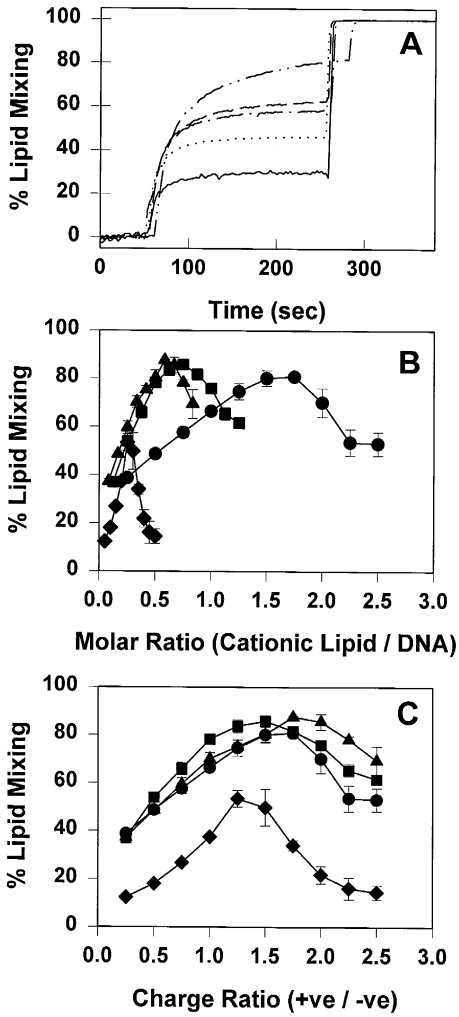

Fig. 9. Kinetics and final extent of DNA-induced lipid mixing of cationic lipids using pyrene-PE. (A) Kinetics of pDNA-induced mixing of DMRIE liposomes. Samples contained 10 μM cationic lipid. 50 μl of DNA at the appropriate concentration to obtain the desired lipid:DNA charge ratio was injected at $t = 50$ s. Charge ratios employed were: (——) 0.25:1, (· · · · · ·) 0.50:1, (——·——) 0.75:1, (—— ——) 1.0:1, (——·· ——) 1.25:1. Detergent was added at 250 s to provide a value for complete lipid mixing. Final extent of pDNA-induced lipid mixing as a function of (B) molar ratio and (C) the apparent charge ratio of cationic lipid:DNA for (●) DMRIE, (■) #43, (▲) #47, and (♦) DOSPA. Error bars represent standard deviations.

Dextran layers. At low charge ratios, the lipid:DNA complex band on top of the 20% Dextran layer was relatively small, and free DNA was observed on top of the 5% Dextran layer. As the charge ratio of cationic lipid:DNA was increased, the band of lipid:DNA complex on top of the 20% Dextran layer increased in size and the amount of free DNA decreased. In agreement with the agarose gel results (Fig. 5), free DNA was observed until a charge ratio of lipid:DNA of 1.0:1 was attained. At a charge ratio of 1.5:1, the band on top of the 20% Dextran layer was no longer observed and a new band was seen on top of the 10% Dextran layer, along with the band on top of the 15% layer. Increasing the charge ratio to 2.5:1 resulted in all the complex banding on top of the 10% Dextran layer; free lipid was observed again on top of the 5% Dextran layer. Thus, these data indicate the presence of multiple forms of the cationic lipid:pDNA complex at all charge ratios, and the predominant species sedimented less well as the lipid:pDNA ratio was increased, indicating lower density, larger size, or both.

Complexes formed using lipid 43 (net charge +2) liposomes migrated to the top of the 30% Dextran

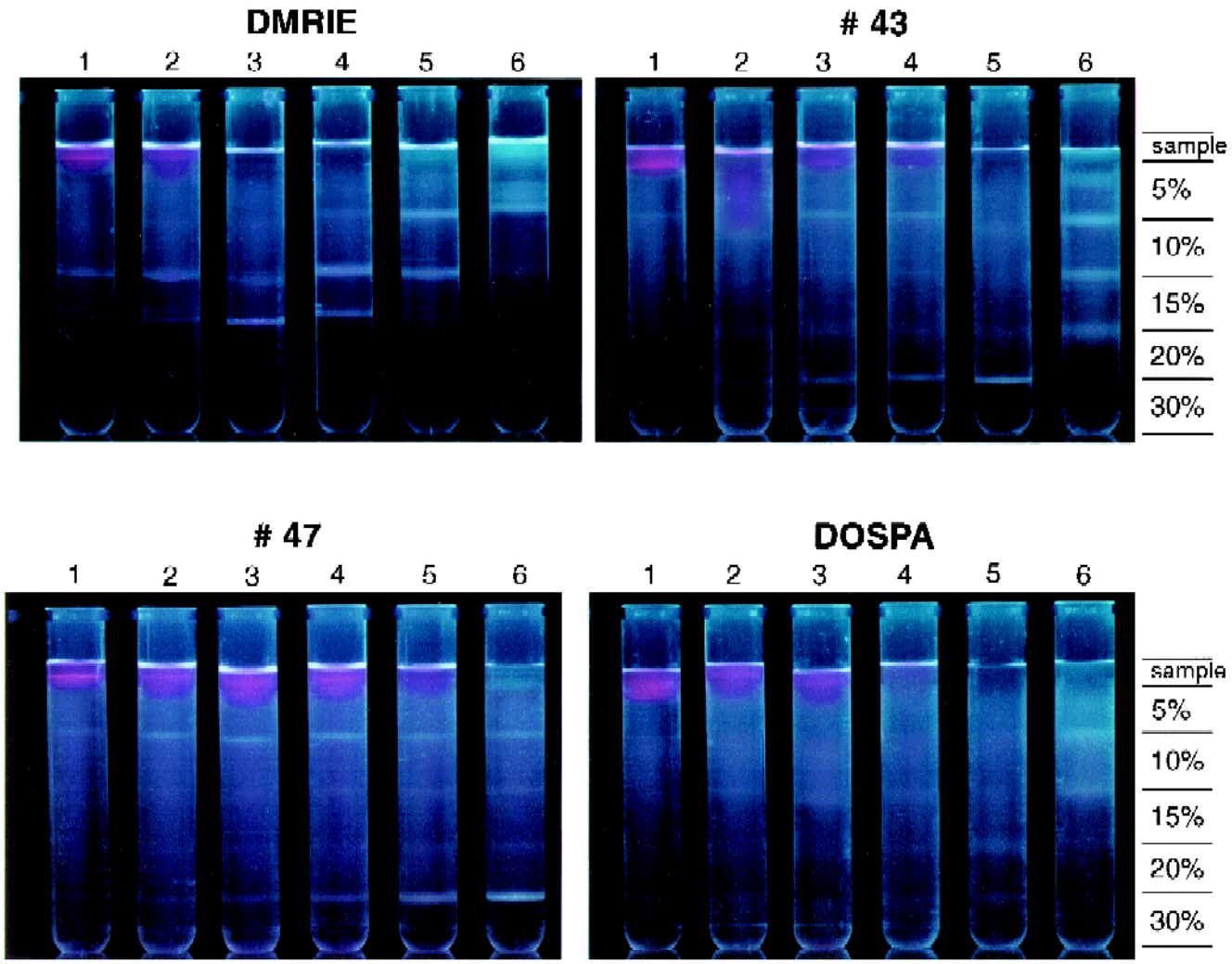

Fig. 10. Dextran T-500 step gradient analysis of cationic lipid:DNA complexes formed from different cationic lipids at various charge ratios of lipid:DNA. Cationic lipid:DOPE vesicles were labeled with Pyrene-PE; pDNA was visualized with EtBr (see Section 2 for additional details). Apparent charge ratios employed for all cationic lipids were: (1) 0.25:1, (2) 0.50:1, (3) 0.75:1, (4) 1.00:1, (5) 1.50:1, and (6) 2.50:1.

layer, indicating that they were smaller or more dense than the DMRIE complexes. A higher density for these complexes might be predicted, since each liposome formed from the divalent lipid 43 should bind twice the amount of DNA as a DMRIE liposome [14]. This notion is supported by the particle sizing data indicating that lipid 47 complexes are similar in size to DMRIE complexes, but move further into the gradient. Free DNA was observed in the samples containing lipid at charge ratios $\leq$ 1.0:1. At a charge ratio of 1.5:1, all the DNA was complexed, and all the DNA and lipid were found on top of the 30% Dextran layer. At a charge ratio of 2.5:1, enough lipid was present to increase the size or buoyancy of the complex, as demonstrated by the coincidental disappearance of the band on top of the 30% Dextran layer and appearance of multiple bands at the interfaces of each of the less dense Dextran layers. The heterogeneity of lipid:DNA complexes formed at high lipid to DNA ratios was well illustrated in this sample.

Lipid 47 (net charge +3) liposomes produced complexes that also banded on top of the 30% Dextran layer. Consistent with all the previous data, it required more lipid 47 (on a charge ratio basis) to complex all the DNA; free DNA was observed even at a charge ratio of 1.5:1. The majority of the lipid 47:DNA complexes were found on top of the 30% interface even at a charge ratio of 2.5:1. However, weak bands were observed at the 10%, 15%, and 20% Dextran interfaces, testifying to the heterogeneity of the complexes formed at this ratio. The apparent greater density of the lipid 47 complexes compared to those formed from DMRIE and lipid 43 might be attributable to the smaller amount of the +3 lipid (#47) required to obtain the same charge ratio.

DOSPA (net charge +5) liposomes complexed with DNA pelleted through the 30% Dextran layer, making them difficult to photograph. Free DNA was observed only at charge ratios of 1.0 and below. No complex bands were observed at these charge ratios as the complexes were either so small or dense that they pelleted through the 30% Dextran layer. It was not possible to prepare Dextran solutions at the higher concentrations necessary to trap these complexes. Very faint bands were observed on top of the 10% and 15% Dextran layers at a charge ratio of 2.5:1, but the majority of the complex pelleted to the bottom of the tube.

4. Discussion

We have examined the biophysical properties of the complexes formed from four model cationic lipids and pDNA. The model cationic lipids were chosen such that the net positive headgroup charge varied between +1 and +5 (see Fig. 1). Although there were similarities in their structures, e.g., all had diacyl chains, there were also significant differences, such as the structure of the linkers and headgroups. Given the fact that the interaction between cationic liposomes and pDNA was expected to be dominated by ionic interactions, it was anticipated that the biophysical attributes of the lipid:pDNA complexes formed from any one cationic lipid would depend strongly on the apparent charge ratio of the positive charges of the cationic amines and the negative charges of the pDNA phosphates. What could not be predicted, and what these data reveal, is that these attributes are very similar at identical charge ratios for *all* of the model cationic lipids, regardless of the number of charges on the cationic lipid headgroup. For example, it was found that zeta potentials of the complex (Fig. 3), EtBr exclusion (Fig. 7), and pDNA-induced lipid mixing (Fig. 9) as a function of the cationic lipid:pDNA ratio were essentially identical for all of the model lipids when the data were expressed as a function of the cationic lipid:pDNA charge ratio. This result thus not only demonstrates the importance of charge–charge interactions in the formation and properties of the complex, but implies that these interactions are dominant over other structural features of the lipids in determining these biophysical attributes of the complex.

In the face of these charge-dominated similarities, it is also true that the different model cationic lipids form complexes that exhibit some significant physical differences. This fact probably is best illustrated by the dextran step gradient results (Fig. 10). Although a heterogeneous mixture of complexes was formed from each the cationic lipids at a given cationic lipid:pDNA ratio, the nature of the complexes formed from each of these model lipids was different as measured by this assay. For a given

cationic lipid, the density of the complexes appeared to decrease as the cationic lipid:pDNA ratio was increased. For example, DMRIE complexes prepared at a charge ratio of 1.5:1 were much larger than those made at a charge ratio of 2.5:1 (by both FFEM and PCS), yet traveled further into the gradient. At a given cationic lipid:pDNA ratio, the sedimentation in the gradient was greater for lipids with more positive charges. For example, at all charge ratios, the multiple complexes formed from DOSPA (+5) sedimented further in the gradient than those formed from DMRIE (+1). These results imply that compared to DMRIE complexes, DOSPA complexes are either smaller, more dense or both. The sizes of DOSPA complexes are certainly smaller than those formed from DMRIE, viz. 126 versus 214 and 424 nm, respectively (see above). Thus, although formation of complexes from the various model cationic lipids is a similar process in that it is driven by charge neutralization and results in a heterogenous mixture of complexes (Fig. 10), the densities or sizes of these complexes are characteristic of the individual cationic lipid.

4.1. Existing models of cationic lipid:DNA complexes

Two fundamentally different types of models have been proposed for cationic lipid:DNA complexes, an 'external' model, in which DNA is adsorbed onto the surface of cationic liposomes [22,28], and a 'internal' model, in which the DNA is surrounded or 'coated' by a lipid envelope [13,21,26,27]. Both models rely on the electrostatic interactions between DNA and cationic lipid to drive the formation of the complex. Although not always stated explicitly, corresponding compaction or condensation of both the lipid and DNA as a result of these ionic interactions is likely to occur. Given these two types of models, it is worth examining at the outset the experimental data in the literature that supports them.

An external model consisting of four cationic liposomes interacting with each plasmid was proposed based on (i) (unpublished) light scattering results indicating a slight size increase of the complex compared to the starting liposomes, (ii) a calculation of the number of positive charges per liposome, and (iii) an assumption of complete charge neutralization for complex formation [28]. Based on the calculation of the number of cationic lipids per vesicle, and the fact that the authors refer to sonicated vesicles, it is most likely that this model was based on vesicles of an average diameter of 25 nm, not the 250 nm reported [28]. For vesicles with an average diameter of 250 nm, a reasonable estimate of the number of cationic lipids/vesicle would be $\approx 280\,000$ [1] not the 1250 reported [28]. Thus, a more realistic external model based on neutralization of the cationic charges, would feature multiple plasmids adsorbed onto each liposome, e.g., approximately 20 plasmids of 7.2 kb in this example, assuming that the cationic lipids contained on the inner monolayer of the vesicles would flip-flop during lipid mixing. Such a model has been proposed for the interaction of TMV-RNA with cationic liposomes (model II of Ballas et al. [25]).

Experimental support for a model of the complex in which lipid 'coats' the DNA comes in large part from electron microscopy results. Freeze-fracture electron microscopic results have shown the presence of some filamentous strands of the appropriate size for a lipid ensheathed DNA strand [21]. However, since free DNA is not visualized employing this technique, it is unclear what fraction of the DNA is involved in such structures. Cryo-transmission electron microscopic images have been interpreted as representing multilamellar structures in which the DNA is trapped between the lamellae, although the authors also state that the images may represent condensed DNA on the surface of the vesicles [29]. In addition, complexes prepared with an excess of negative charge showed DNA protruding from the surface of the complexes [29], consistent with our data indicating that complexes prepared with excess DNA have negative zeta potentials (Figs. 3 and 4). Cationic lipid:DNA structures with DNA protruding from the surface are clearly visible in rotary shadowed negatively stained electron micrographs [20], even though these complexes were prepared at a

[1] For a 250 nm vesicle, the surface area is $2.0 \cdot 10^7$ Å^2. If the surface area of a lipid head group is estimated at 70 Å^2, and 50% of the lipids are cationic, then each vesicle should contain $(2.0 \cdot 10^7/70)/2 = 1.4 \cdot 10^5$ cationic lipids/leaflet or 280 000 cationic lipids/bilayer.

molar ratio of approximately 1.20 cationic lipids (DMRIE):1 nucleotide. Such structures are more consistent with an external model of a lipid core surrounded by DNA, than with models in which it is proposed that the DNA is encapsulated within a lipid bilayer.

The ability of DNA to induce lipid mixing between cationic liposomes [17,18,20] has also been used to support a model in which the DNA is encapsulated within a lipid coat. However, lipid mixing is predicted by both an external (bound) or internal (encapsulated) model of cationic lipid:DNA complexes, and in itself is not conclusive for either model.

Negative staining of cytochrome c coated DNA has been interpreted as evidence that cationic liposomes adsorb to the DNA at lower liposome to DNA ratios as 'beads on a string' that fuse together to ensheath the DNA at higher liposome to DNA ratios [17]. It must be pointed out, however, that the Kleinschmidt procedure used in this study to visualize DNA employs a very high ionic strength buffer (0.5 M NH_4OAc, 0.1 M Tris) together with 2.5 mM EDTA and 0.25 mg/ml cytochrome *c*, a highly basic protein, in solutions that were 0.5 μM DNA (in nucleotides). Given that the predominant interactions between DNA and cationic liposomes are electrostatic in nature, it is highly unlikely that this set of conditions would lead to the same structures that would be formed at low ionic strength, or even at physiologic ionic strength. Note for example, in this same study, the effects of polylysine, an analog of a basic protein, on complex formation between cationic lipids and DNA. Thus, while in toto electron microscopic examinations of the complex may be suggestive of an internal model, they are at present far from conclusive and there is very limited biophysical data reported in the literature to support such structures.

With this in mind, it must be noted that the conditions in which the complex is formed may greatly affect the final structure of the complex. A list of some of the parameters that may affect complex formation can be found in Felgner et al. [26]. In these studies, we have only attempted to identify the characteristics of lipid:DNA complexes that are formed by methods most commonly reported in the literature, that is, a relatively rapid mixing of preformed cationic liposomes with DNA.

4.2. Implications of present results for models of cationic lipid:DNA complexes

4.2.1. FFEM and Dextran gradients

Density gradient profiles and FFEM gave comparative information about the heterogeneity and size of the cationic lipid:pDNA complexes. FFEM of complexes formed from DMRIE demonstrated what appeared to be aggregates of multilamellar structures at all DMRIE:pDNA ratios (Fig. 2). The lamellae of these structures did not appear to be normal, as has been noted previously based on cryo-EM results [29]. Rather, they appeared to be compacted or condensed. It is entirely possible that the pDNA has altered the lipid structure significantly, e.g., it may dehydrate the headgroup region; pDNA certainly causes extensive lipid mixing (Fig. 9). Interestingly, the heterogeneity as well as the size of the structures both appeared to increase with the lipid:pDNA ratio. Although the pDNA was not visualized, these structures appeared to be very similar to those observed recently by cryo-EM [29], in which DNA was visible protruding from the complexes at cationic lipid:pDNA molar ratios less than one.

Lipid:DNA complexes made from the four different cationic lipids as a function of the cationic lipid:pDNA charge ratio were applied to Dextran T-500 step gradients (Fig. 10). Although for each of the model lipids this resulted in multiple bands, and by inference, multiple species of the complex, these complexes behaved similarly for each of the lipids. For a given lipid, as the cationic lipid:DNA ratio was increased, the bands containing complex appeared at lower densities, indicating lower density or larger size of the complex, or both. As the headgroup charge increased at a constant cationic lipid:pDNA ratio, the bands containing complex appeared at higher densities, indicating higher density or smaller size of the complex, or both.

Taken together, the FFEM and Dextran gradient data indicate the formation of heterogenous complexes that become less dense or larger as the lipid:pDNA ratio is increased, but do not provide direct evidence for or against either of the potential models of the complex. At higher cationic lipid:pDNA ratios, the FFEM images appear to show relatively normal vesicular structures aggregated with more condensed structures (see Fig. 2E). These images

may be the result of the adsorption of excess cationic lipid vesicles onto pDNA-coated liposomes, and provide some indirect support for an external model of the complex.

4.2.2. Gel migration and lipid mixing

The gel migration and lipid mixing data provide information regarding the effects of cationic liposomes on pDNA and the effects of pDNA on cationic liposomes, respectively. The gel retardation data (Fig. 5) indicate that a DNA molecule either migrates as a free molecule or it interacts with a liposome in such a way that it remains in the well, either due to charge neutralization, an increase in size, or both. The fact that the gel profiles were similar for each of the model cationic lipids argues simply that liposomal retardation of DNA is equivalent for equivalent charge neutralization, regardless of the structure of the cationic lipid.

DNA was shown to induce relatively rapid lipid mixing between cationic liposomes (Fig. 9A), in agreement with previously reported results [17,18,35]. The results presented here indicate that similar initial rates of lipid mixing were induced by each of the four model lipids as a function of charge ratio, i.e., the rate of lipid mixing was found to be independent of the net charge on the lipid headgroup or the detailed structure of the lipid. At all lipid:DNA ratios tested, the majority of the lipid mixing occurred within 30 s following DNA addition.

The presence of free liposomes, such as observed in Dextran gradients of complexes formed at high charge ratios ($\geq$ 1.5:1 for DMRIE liposomes), provides a partial explanation as to why the apparent extent of lipid mixing decreased when the charge ratio exceeded $\approx$ 1.5:1. Binding of excess cationic liposomes without lipid mixing, i.e., aggregation as noted above from the FFEM images, may also be partially responsible for the reduced lipid mixing observed at charge ratios above 1.5:1.

The fact that lipid mixing approached 100% (Fig. 9C) implies that DNA induces not only interbilayer mixing, i.e., between the bilayers of different liposomes, but also induces interleaflet mixing, i.e., the flip-flop rate of cationic lipids in these liposomes is relatively rapid, especially in the presence of DNA. This result is consistent with the observation that we have found cationic liposomes to be extremely permeant (unpublished results). Thus, for example it has been found impossible to trap solutes in DMRIE:DOPE vesicles by standard procedures (unpublished results). In addition the chemical reduction, by dithionite, of all the NBD-labeled lipids in DMRIE:DOPE cationic liposomes is extremely rapid, even those on the inside of the liposome. These observations have important implications for the interaction of the cationic lipid charges with the DNA, as it implies that essentially all of the cationic lipid may be available for interaction with and charge neutralization of the DNA.

The gel migration data are consistent with the cooperative interaction of cationic lipids with pDNA, i.e., a pDNA molecule appears to interact with a large number of cationic lipids or none at all. These data do not directly favor one model of the complex. The lipid mixing data indicate that pDNA induces lipid mixing between liposomes at all cationic lipid:pDNA ratios. This observation reinforces the idea of a cooperative interaction of liposomes induced by pDNA, and further implies a substantial rearrangement of lipids as a result. Whether this rearrangement signifies the formation of an internal or external complex is unclear.

4.2.3. EtBr accessibility

One deduction that has been made based on previous EtBr accessibility experiments is that a ‘critical point’ in the formation of the cationic lipid:DNA complex exists around charge neutrality [17]. However, as we have demonstrated in Fig. 6, this apparent critical point behavior is a result of a limiting amount of EtBr relative to DNA rather than to a critical point in the process of complex formation. In reality, as Fig. 6 shows, EtBr accessibility is a monotonic function of cationic lipid:DNA ratio. Thus, the EtBr accessibility data, when EtBr is not limiting, support a model in which the accessibility of DNA to EtBr is gradually decreased as the amount of cationic lipid is increased. These data would appear to be consistent with a gradual encapsulation of the DNA by lipid. However, the fact that polylysine interacts with DNA and excludes EtBr with precisely the same charge ratio profile (data not shown), argues that charge neutralization of DNA and its resulting condensation [15,36,37] is sufficient to prevent EtBr intercalation. Thus, ensheathing DNA within a hydrophobic lipid

envelope in an internal model as has been suggested [17,21] is not necessary to prevent EtBr intercalation. The EtBr exclusion results shown in Fig. 6 are also entirely consistent with an external model in which DNA is *compacted* as a result of its interaction with the cationic liposome. The observed EtBr fluorescence would then be directly related to the fraction of the DNA that remained unbound, which in turn would be inversely related to the cationic lipid:DNA ratio.

Higher ionic strength appears to increase the accessibility of DNA in the complex to EtBr, as demonstrated by the data in Fig. 8. This increased accessibility to EtBr at higher ionic strength does not appear to be due to a dissociation of the DNA from the complex, since the gel retardation data (Fig. 5), which are determined at moderate ($\approx$ 100 mM Tris/borate) ionic strength show that the DNA is entirely bound to lipid, especially at high lipid to DNA ratios. These data can be used to support an external model if one assumes that the effects of salt are to decrease the association of the DNA with the cationic liposome, and thereby decrease the compaction of the DNA, allowing for EtBr intercalation. In an internal model, the effect of salt could be rationalized by an effect on lipid packing, allowing EtBr more access to the coated DNA at higher ionic strength. However, it is worth noting, as stated above, that cationic liposomes in general appear to be extremely permeant to small solutes.

4.2.4. Zeta potentials

Zeta potentials of the four model cationic lipids complexed with DNA at different ratios of lipid to DNA indicated that the lipid:DNA complexes formed had very similar surface characteristics at the same apparent charge ratio of cationic lipid:DNA (Fig. 3). At charge ratios ≤ 1, i.e., when DNA was in charge excess, the zeta potentials of the complexes in 1mM NaCl were negative and essentially independent of the charge ratio for all the lipids tested (Fig. 3). Given the caveat that the zeta potentials determined are likely to be averages of multiple species of complex, these results are consistent with an external model in which DNA, when it is in charge excess, binds maximally to all available liposomes. It is difficult to reconcile these data with an internal model, e.g., beads on a string, since the zeta potentials in such a model would be predicted to become *progressively* more positive with increases in the lipid:DNA ratio.

It should be noted that the zeta potentials of complexes formed at charge ratios below 1:1, i.e., negatively charged, had on average a much smaller width than those of complexes formed above this ratio (data not shown). In other words, complexes formed in the presence of excess liposomes (positively charged complexes) were relatively more heterogeneous than those formed in excess DNA. This observation is consistent with the FFEM results (Fig. 2). These data are also consistent with an external model, in which at low cationic lipid:pDNA ratios the liposomes are coated with pDNA that prevents aggregation and results in a relatively homogenous population of complexes, and at high ratios pDNA-coated liposomes are involved in aggregates with excess liposomes.

Increasing the ionic strength of the medium had several effects on the zeta potentials of the complexes. In terms of an internal model, these effects of ionic strength are difficult to rationalize, e.g., the zeta potential at high lipid:pDNA ratio should be determined by the cationic lipid, which would not result in a negative zeta potential (see Fig. 4). In terms of an external model the more negative zeta potentials of the complexes at higher ionic strength may be the result of weaker binding of DNA to the surface of the cationic liposome resulting in an extension of the DNA from the liposome surface, as shown schematically in Fig. 11. Due to the multiple valences of both liposome and DNA, the DNA would not completely dissociate from the liposome, but portions of the DNA would on average spend more time at a greater distance from the liposome surface than would be the case in a lower ionic strength buffer. Thus, at low ionic strength the DNA would bind tightly to the surface of the liposome and many of its negative charges would be neutralized. In contrast, in a higher ionic strength medium, the DNA would extend from the liposome surface and resemble an anionic cloud similar to the neutral clouds proposed for polyethylene glycol-coated liposomes by Torchilin et al. [38]. This anionic DNA cloud would shield the positive charges on the liposome surface without being neutralized by direct interaction with the cationic lipid. Thus, the effective surface of the liposome, i.e., that measured by the zeta potential, would be at least

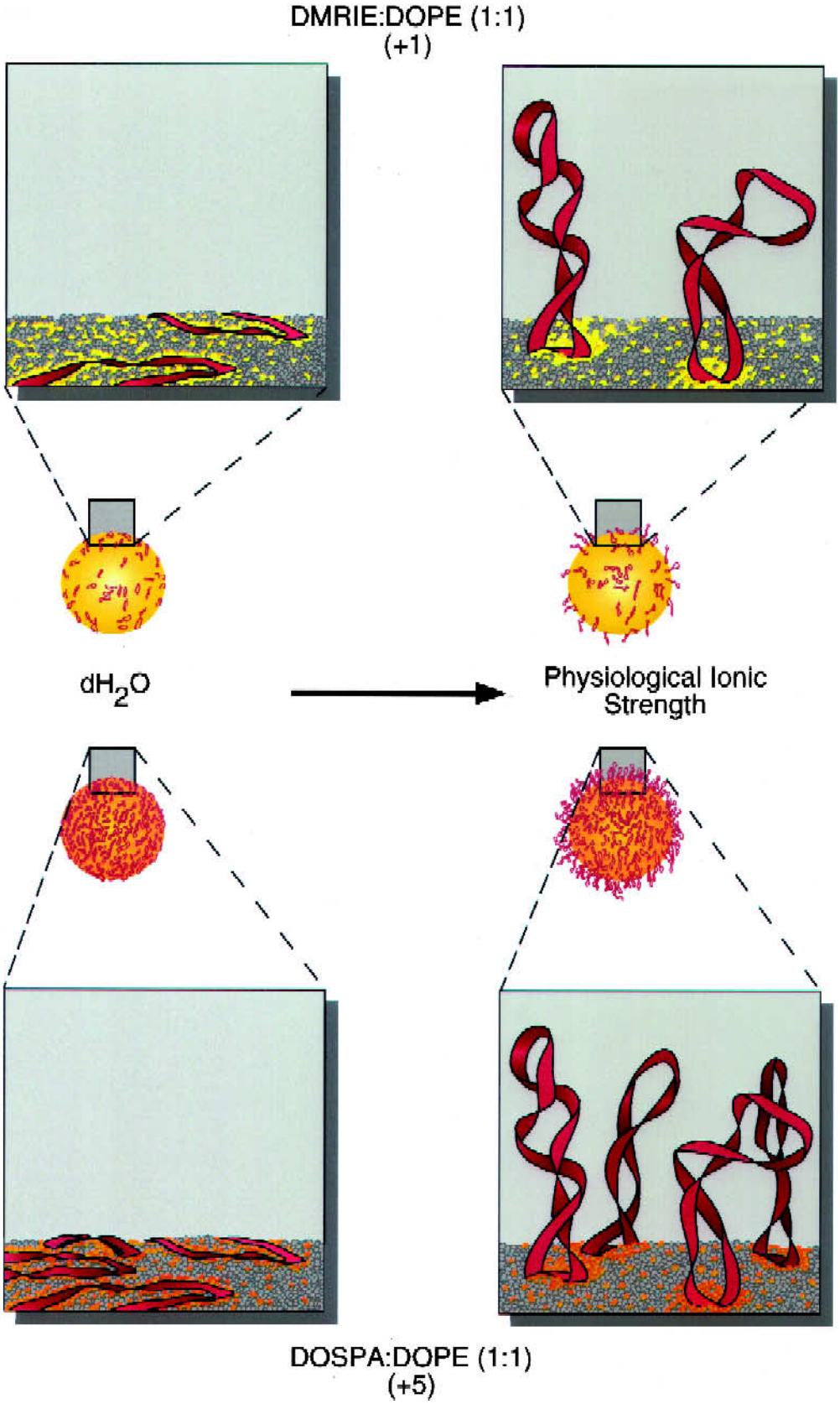
DMRIE:DOPE (1:1)
(+1)
dH2O
Physiological Ionic Strength
DOSPA:DOPE (1:1)
(+5)

in part, the extended, highly negative DNA cloud. This hypothesis is consistent with the EtBr exclusion results (performed in 150 mM NaCl) which indicated that 55% of the DNA was still accessible to EtBr even when DMRIE was present a charge ratio of 2.0:1, conditions under which all the DNA was bound to liposomes as evidenced by agarose gel electrophoresis (Fig. 5).

A second effect of high ionic strength, namely the increased amount of cationic lipid required to change the sign of the zeta potential on the complex (see Fig. 4), may also be accounted for by a reduction in the strength of the lipid:DNA interaction in an external model in the presence of salt. Neutralization of the negative charges on a DNA cloud at high ionic strength would require additional lipid.

4.3. Summary

Our zeta potential analysis and EtBr intercalation studies at low lipid:DNA charge ratios in the presence of NaCl are most consistent with the interpretation that the majority of the DNA is bound to the exterior of the complex and not encapsulated within a lipid coat. Analysis of the complexes by FFEM is complicated by the fact that free DNA cannot be observed by this technique. Recent results reported by Gustafsson et al. [29], employing cryo-TEM (a method in which free DNA can be seen), showed DNA protruding from complexes formed at low lipid:DNA ratios, a finding that supports an external model. In addition, work by Jääskeläinen et al. [18], showed that complexes formed with excess cationic lipid induced leakage from anionic (DPPC/DPPG) liposomes containing calcein, but that complexes prepared with excess DNA (on a charge basis) did not result in release of vesicle contents. The authors attributed this to the production of an anionic complex that did not interact with the anionic liposomes, i.e., an external model.

Finally, it is useful to consider the implications of these results in terms of the interactions of cationic lipid:DNA complexes with the target cell. One clear result from these data is that apparent cationic lipid:DNA charge ratios of $\geq 1.5{:}1$ are necessary to produce a complex with an overall net positive charge, as shown by the zeta potential measurements in Fig. 3. If the initial interaction of lipid:DNA complexes with the cell is driven primarily by electrostatics, this result would imply that maximal interaction and possibly maximal uptake would occur at charge ratios $\geq 1.5{:}1$. However, it should be noted that relatively efficient transfection of cells has been observed at charge ratios of cationic lipid to DNA that should carry a net negative charge according to our results (see as an example Refs. [39,40]). This suggests that the initial surface charge of the complex may serve an indirect purpose other than direct interaction with the cell surface, e.g., adsorption of proteins. Potentially more important roles of the cationic lipid may be to compact the DNA or to aid in its escape from an endosomal compartment rather than to impart charge to the complex.

Acknowledgements

We wish to thank Phil Felgner of Vical Inc., for providing DMRIE and DOSPA, and Maribeth Cherry, Nick Wan, Dave McNeilly and Nelson Yew for providing the purified plasmid DNA.

References

[1] Felgner, P.L., Gadek, T.R., Holm, M., Roman, R., Chan, H.W., Wenz, M., Northrop, J.P., Ringold, G.M. and

Fig. 11. Schematic diagram of proposed effect of ionic strength on the structure of cationic lipid:DNA complexes formed from monovalent and multivalent cationic lipids. At low ionic strength, DNA binds tightly to the surface of the cationic vesicles, neutralizing many of the charges on the DNA. At increased ionic strength, a proportion of the DNA is displaced from the vesicle surface and forms an anionic cloud around the cationic lipid core. The DNA shields the positive charges of the cationic lipid without being neutralized by the lipid, giving the complex a more negative zeta potential in high ionic strength buffer than in low ionic strength buffer. Complexes prepared with multivalent cationic lipids have a higher density of plasmids/lipid vesicle so that more positive charges are shielded by the DNA cloud. More multivalent cationic lipid than monovalent cationic lipid is therefore required to neutralize all the DNA when the complexes are in a high ionic strength environment. Grey headgroups represent DOPE, colored headgroups represent the cationic lipids.

Danielsen, M. (1987) Proc. Natl. Acad. Sci. USA 84, 7413–7417.
[2] Brigham, K.L., Meyrick, B., Christman, B., Magnuson, M., King, G. and Berry, L.C. Jr. (1989) Am. J. Med. Sci. 298, 278–281.
[3] Stribling, R., Brunette, E., Liggitt, D., Gaensler, K. and Debs, R. (1992) Proc. Natl. Acad. Sci. USA 89, 11277–11281.
[4] Alton, E.W.F.W., Middleton, P.G., Caplen, N.J., Smith, S.N., Steel, D.M., Munkonge, F.M., Jeffery, P.K., Geddes, D.M., Hart, S.L., Williamson, R., Fasold, K.I., Miller, A.D., Dickinson, P., Stevenson, B.J., McLachlan, G., Dorin, J.R. and Porteous, D.J. (1993) Nature Genetics 5, 135–142.
[5] Nabel, G.J., Nabel, E., Yang, Z.-Y., Fox, B.A., Plautz, G.E., Gao, X., Huang, L., Shu, S., Gordon, D. and Chang, A.E. (1993) Proc. Natl. Acad. Sci. USA 90, 11307–11311.
[6] Conary, J.T., Parker, R.E., Christman, B.W., Faulks, R.D., King, G.A., Meyrick, B.O. and Brigham, K.L. (1994) J. Clin. Invest. 93, 1834–1840.
[7] Yoshimura, K., Rosenfeld, M.A., Nakamura, H., Scherer, E.M., Pavirani, A., Lecocq, J.P. and Crystal, R.G. (1992) Nucleic Acids Res. 20 (12), 3233–3240.
[8] Gao, X. and Huang, L. (1991) Biochem. Biophys. Res. Commun. 179, 280–285.
[9] Rose, J.K., Buonocore, L. and Whitt, M.A. (1991) Biotechniques 10, 520–525.
[10] Kamata, H., Yagisawa, H., Takahashi, S. and Hirata, H. (1994) Nucleic Acids Res. 22, 536–537.
[11] Philip, R., Brunette, E., Kilinski, L., Murugesh, D., McNally, M.A., Ucar, K., Rosenblatt, J., Okarma, T.B. and Lebkowski, J.S. (1994) Mol. Cell. Biol. 14, 2411–2418.
[12] Pickering, J.G., Jekanowski, J., Weir, L., Takeshita, S., Losordo, D.W. and Isner, J.M. (1994) Circulation 89, 13–21.
[13] Barthel, F., Remy, J.-S., Loeffler, J.-P. and Behr, J.-P. (1993) DNA Cell Biol. 12, 533–650.
[14] Singhal, A. and Huang, L. (1994) Gene Therapy: From Basic Research to the Clinic (K.M. Hui, ed.), pp. 107–129, World Scientific Publishing Co., Singapore.
[15] Behr J-P. (1994) Bioconj. Chem. 5, 382–389.
[16] Felgner, J.H., Kumar, R., Sridhar, C.N., Wheeler, C.J., Tsai, Y.J., Border, R., Ramsey, P., Martin, M. and Felgner, P.L. (1994) J. Biol. Chem. 269, 2550–2561.
[17] Gershon, H., Ghirlando, R., Guttman, S.B. and Minsky, A. (1993) Biochemistry 32, 7143–7151.
[18] Jääskeläinen, I., Mönkkönen, J. and Urtti, A. (1994) Biochim. Biophys. Acta 1195, 115–123.
[19] Maccarrone, M., Dini l., Di Giulio, A., Rossi, A., Giuseppe, M. and Finazzi-Agro, A. (1992) Biochem. Biophys. Res. Commun. 186, 1417–1422.
[20] Zabner, J., Fasbender, A.J., Moninger, T., Poellinger, K.A. and Welsh, M.J. (1996) J. Biol. Chem. 270, 18997–19007.
[21] Sternberg, B., Sorgi, F.L. and Huang, L. (1994) FEBS Lett. 356, 361–366.
[22] Behr, J-P. (1986) Tetrahedron Lett. 27, 5861–5864.
[23] Bertling, W., Gares, M., Paspaleeva, V., Zimmer, A., Kreuter, J., Nürnberg, E. and Harrer, P. (1991) Biotech. Appl. Biochem. 13, 390–405.
[24] Kabanov, A.V. and Kabanov, V.A. (1995) Bioconj. Chem. 6, 7–20.
[25] Ballas, N., Zakai, N., Sela, I. and Loyter, A. (1988) Biochim. Biophys. Acta 939, 8–18.
[26] Felgner, P.L., Tsai, Y.J., Sukhu, L., Wheeler, C.J., Manthorpe, M., Marshall, J. and Cheng, S.H. (1995) Ann. NY Acad. Sci. 772, 126–139.
[27] Felgner, P.L, Tsai, Y.J. and Felgner, J.H. (1996) in Handbook of Non-Medical Applications of Liposomes (Lasic, D.D. and Barenholz, Y., eds.), pp. 43–56, CRC Press, New York.
[28] Felgner, P.L. and Ringold, G.M. (1989) Nature (Product Review) 337, 387–388.
[29] Gustafsson, J., Arvidson, G., Karlsson, G. and Almgren, M. (1995) Biochim. Biophys. Acta 1235, 305–312.
[30] Aida, Y. and Pabst, M.J. (1990) J. Immunol. Methods 132, 191–195.
[31] Fisher, K. and Branton, D. (1974) Methods Enzymol. 32, 35.
[32] Bron, R., Wahlberg, J.M., Garoff, H. and Wilschut, J. (1993) EMBO J. 12, 693–701.
[33] Nieva, J.L., Bron, R. Corver, J. and Wilschut, J. (1994) EMBO J. 13, 2797–2804.
[34] Zhou, X., Klibanov, A.L. and Huang, L. (1991) Biochim. Biophys. Acta 1065, 8–14.
[35] Düzgünes, N., Goldstein, J.A., Friend, D.S. and Felgner, P.L. (1989) Biochemistry 28, 9179–9184.
[36] Manning, G.S. (1980) Biopolymers 19, 37–59.
[37] Wagner, E., Cotten, M., Foisner, R. and Birnstiel, M.L. (1991) Proc. Natl. Acad. Sci. USA 88, 4255–4259.
[38] Torchilin, V.P., Omelyaneku, V.G., Papisov, M.I., Bogpanon, A.A. Jr., Trubetskoy, V.S., Herron, J.N. and Gentry, C.A. (1994) Biochim. Biophys. Acta 1195, 11–20.
[39] Lee, R.L., Marshall, J., Siegel, C.S., Jiang, C., Yew, N.S., Nichols, M.R., Nietupski, J.B., Ziegler, R.J., Lane, M., Wang, K.X., Wan, N.C., Scheule, R.K., Harris, D.J., Smith, A.E. and Cheng, S.H. (1996) Human Gene Therapy, accepted for publication.
[40] Fasbender, A.J., Zabner, J. and Welsh, M.J. (1995) Am. J. Physiol. 269 (13), L45–L51.